

# Learning Embedding Adaptation for Few-Shot Learning

Han-Jia Ye\*  
 Nanjing University  
 Nanjing, China, 210023  
 yehj@lamda.nju.edu.cn

Hexiang Hu  
 USC  
 Los Angeles, CA 90089  
 hexiangh@usc.edu

De-Chuan Zhan  
 Nanjing University  
 Nanjing, China, 210023  
 zhandc@lamda.nju.edu.cn

Fei Sha<sup>†</sup>  
 Netflix  
 Los Angeles, CA 90028  
 fsha@netflix.com

## Abstract

*Learning with limited data is a key challenge for visual recognition. Few-shot learning methods address this challenge by learning an instance embedding function from seen classes, and apply the function to instances from unseen classes with limited labels. This style of transfer learning is task-agnostic: the embedding function is not learned optimally discriminative with respect to the unseen classes, where discerning among them is the target task. In this paper, we propose a novel approach to adapt the embedding model to the target classification task, yielding embeddings that are task-specific and are discriminative. To this end, we employ a type of self-attention mechanism called Transformer to transform the embeddings from task-agnostic to task-specific by focusing on relating instances from the test instances to the training instances in both seen and unseen classes. Our approach also extends to both transductive and generalized few-shot classification, two important settings that have essential use cases. We verify the effectiveness of our model on two standard benchmark few-shot classification datasets — MiniImageNet and CUB, where our approach demonstrates state-of-the-art empirical performance.*

## 1. Introduction

Learning visual recognition systems with deep learning architectures [14, 19, 38] often starts with annotating a large number of labeled images from a set of pre-defined visual categories [9, 27, 49]. Despite its utility, such a paradigm

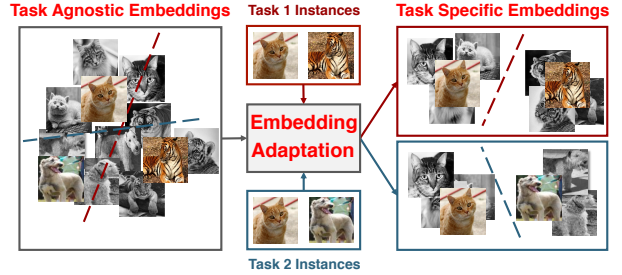


**Figure 1:** An illustration of the Embedding Adaptation notion. The gray-scaled and colorful images are instances from SEEN and UNSEEN classes respectively. Instead of using task-agnostic embedding, we propose to adapt embedding for each few-shot task.

encounters difficulty in use cases where one needs to learn new visual concepts with limited annotation. For instance, in visual search of merchandises, the search algorithm has access only to a limited set of stock photos (provided by the merchants) for newly released products.

To this end, few-shot learning has emerged as a promising approach in tackling this challenge [10, 20, 21, 24, 44]. Concretely, few-shot visual recognition distinguishes two sets of visual concepts: SEEN and UNSEEN ones. The target task is to construct visual classifiers to identify classes from the UNSEEN where each class has only a very small number of exemplars (“few-shot”). The main idea is to discover transferable visual knowledge in the SEEN classes, which have ample labeled instances, and leverage it to construct the desired classifier. For example, state-of-the-art approaches for few-shot learning [37, 39, 42, 44] usually learn a discriminative instance embedding model from the SEEN categories, and apply the embedding model to visual data in UNSEEN categories. In this common embedding space, non-parametric classifiers (e.g. nearest neighbor

\*This work is mostly performed while Han-Jia Ye was a visiting scholar at USC.

<sup>†</sup>On leave from University of Southern California (feisha@usc.edu).

bors) are then used to avoid learning complicated recognition models from a small number of examples.

Such approaches do suffer from an important limitation. Assuming a common embedding space implies that the discovered knowledge – discriminative visual features – on the SEEN classes are equally effective for *any* UNSEEN classes. In concrete words, suppose we have two different target tasks: discerning “cat” versus “dog” and discerning “cat” versus “tiger”. Intuitively, each task uses a different set of discriminative features. Thus, the most desired embedding model first needs to be able to extract discerning features for either task at the same time. This could be a challenging aspect in its own right as the current approaches are agnostic to what those “downstream” target tasks are and could accidentally de-emphasize selecting features for future use. Secondly, even if both sets of discriminative features are extracted, they do not necessarily lead to the optimal performance for a *specific* target task. The most useful features for discerning “cat” versus “tiger” could be irrelevant and noise to the task of discerning “cat” versus “dog”!

What is lacking in the current approaches for few-shot learning is an *adaptation* strategy that tailors the visual knowledge extracted from the SEEN classes to the UNSEEN ones in a target task. In other words, we desire separate embedding spaces where each one of them is customized such that the visual features are most discriminative for a given task. Figure 1 schematically illustrates this notion.

Towards this, we propose a new few-shot learning approach in this paper. The approach implements the above-mentioned adaptation strategy. Specifically, the adaptation algorithm transforms the embedding models derived from the SEEN classes, leveraging the few labeled instances in the target task. The transformation is obtained with a self-attention architecture called Transformer [25, 43], widely used in natural language processing and more recently in computer vision [31]. The self-attention mechanism enables learning the embedding transformation by considering the relationship among the labeled instances in the target task as well as considering the relationship between the classes in the target task and the SEEN classes. (More detailed discussions are in Section 4.)

Our contribution consists of 3 parts. In Section 4, we describe a meta-learning flavored general framework for adapting representation to specific tasks – the representation can be learnt with any existing approaches. We then evaluate the proposed approach on the standard few-shot learning benchmark datasets (*MiniImageNet* and *CUB*) and demonstrate superior performances (Section 6). Finally, we consider new few-shot learning settings (such as transductive and generalized few-shot learning) which are also important real-world use cases and shown that our approach can outperform baseline algorithms under these settings too.

## 2. Related Work

Learning with limited annotation has been drawing a lot of interests in challenging application scenarios where traditional supervised learning approaches demand a large amount of labeled data. A standard approach is to pre-train models on datasets with ample labels and fine tune the models with a small amount of labeled data from the target task. However, the few-shot learning setting we investigate in this paper has more meager amount of labels (such as 1 or 5 instances per visual concept). Thus, the pre-train strategy often fails, by either significantly overfitting on the target task or updating the pre-trained models very little (and not being able to incorporate inductive bias from the target task).

Zero-shot learning (ZSL) is closely related to few-shot learning [1, 5, 22]. Similarly, ZSL distinguishes SEEN and UNSEEN classes. The main difference is that ZSL does not provide visual exemplars for the UNSEEN classes. Instead, the target tasks provide the semantic connections among the visual concepts in both SEEN and UNSEEN ones. Through those semantic relations, visual classifiers optimized on the SEEN classes are transferred to the UNSEEN ones.

Methods specifically designed for few-shot learning fall broadly into two categories. The first is to control how a classifier for the target task should be constructed. One fruitful idea is the meta-learning framework where the classifiers are optimized *in anticipation* that a future update due to data from a new task performs well on that task [2, 10, 23, 29, 33, 37], or the classifier itself is directly meta-predicted by the new task data [32, 47].

Another line of approach has focused on learning generalizable instance embeddings [1, 5, 6, 18, 28, 42, 44] and uses those embeddings on simple classifiers such as nearest neighbor classification rules. The key assumption is that the embeddings capture all necessarily discriminative representations of data such that simple classifiers are sufficed, hence avoiding the danger of overfitting on a small number of labeled instances. Early work such as [18] first validated the importance of embedding in one-shot learning, whilst [44] proposes to learn the embedding with a soft nearest neighbor objective, following a meta-learning routine. Recent advances have leverages different objective functions for learning such embedding models, *e.g.* considering the class prototype [39], decision ranking [42], and similarity comparison [41]. Most recently, [11] utilizes the graph convolution network [17] to unify the embedding learning.

Our work follows the second school of thoughts. The main difference is that we do not assume the embeddings learned on SEEN classes, being agnostic to the target tasks, are necessarily discriminative for those tasks. In contrast, we propose to *adapt* those embeddings for each target task so that the transformed embeddings are better aligned with the discrimination needed in those tasks. We show empirically that such task-specific embeddings perform better than

task-agnostic ones.

### 3. Few-Shot Learning for Visual Recognition

In this section, we describe the standard formulation of few-shot learning (FSL) for visual categorization [10, 39, 44]. We also introduce two variants: transductive FSL [26, 35] and generalized FSL [46]. There are many use cases of such settings and both are studied in this paper.

**Standard formulation of FSL.** A  $M$ -shot  $N$ -way classification task contains  $N$  classes sampled from a set of visual concepts  $\mathcal{U}$  and  $M$  (training) examples per class. We denote the training set (sometimes referred as support sets in literature) as  $\mathcal{D}_{\text{train}} = \{\mathbf{x}_i, \mathbf{y}_i\}_{i=1}^{NM}$ , with the instance  $\mathbf{x}_i \in \mathbb{R}^D$  and the labeling vector  $\mathbf{y}_i \in \{0, 1\}^N$ . In FSL,  $M$  is often small ( $M = 1$  or  $M = 5$  in this work). The goal is to find a function  $f$  that labels a test instance  $\mathbf{x}_{\text{test}}$ ,

$$\hat{\mathbf{y}}_{\text{test}} = f(\mathbf{x}_{\text{test}}; \mathcal{D}_{\text{train}}) \in \{0, 1\}^N$$

Given the small number of training instances, it is challenging to construct complex classifiers  $f(\cdot)$ . To this end, the learning algorithm is also supplied with additional data consisting of labeled instances. These additional data are drawn from visual classes  $\mathcal{S}$ , which does not overlap with  $\mathcal{U}$ . We refer to the original task as *the target task* which discerns  $N$  UNSEEN classes. To avoid confusion, we denote the data from the SEEN classes  $\mathcal{S}$  as  $\mathcal{D}^{\mathcal{S}}$ .

To learn  $f(\cdot)$  using  $\mathcal{D}^{\mathcal{S}}$ , we synthesize many  $M$ -shot  $N$ -way FSL tasks by sampling the data. Each sampling gives rise to a task to classify  $\mathbf{x}_{\text{test}}^{\mathcal{S}}$  into one of the  $N$  SEEN classes, by learning  $f(\cdot)$  from  $\mathcal{D}_{\text{train}}^{\mathcal{S}}$  composed of the labeled instances on the same set of seen classes. This is similar to the meta-learning framework [10, 44]. Formally, the function  $f(\cdot)$  is learnt to minimize the averaged error over those sampled tasks

$$f^* = \arg \min_f \sum_{(\mathbf{x}_{\text{test}}^{\mathcal{S}}, \mathbf{y}_{\text{test}}^{\mathcal{S}}) \in \mathcal{D}_{\text{test}}^{\mathcal{S}}} \ell(f(\mathbf{x}_{\text{test}}^{\mathcal{S}}; \mathcal{D}_{\text{train}}^{\mathcal{S}}), \mathbf{y}_{\text{test}}^{\mathcal{S}}) \quad (1)$$

where the loss function  $\ell(\cdot)$  measures the discrepancy between the prediction. (For simplicity, we have assumed we only synthesize one task.) The optimal  $f^*$  is then applied to the original target task.

**Transductive FSL.** The key difference between standard and transductive scenario [26, 35] is whether test instances arrive one at a time or all simultaneously. The later setup allows the structure of unlabeled test instances to be utilized. Therefore, the prediction  $f(\mathbf{x}_{\text{test}}; \mathcal{D}_{\text{train}} \cup \mathcal{X}_{\text{test}}) \rightarrow \{0, 1\}^N$  would depend on both training data  $\mathcal{D}_{\text{train}}$  and all available test instances  $\mathcal{X}_{\text{test}} = \{\mathbf{x} ; \forall (\mathbf{x}, \mathbf{y}) \in \mathcal{D}_{\text{test}}\}$ .

### Few-Shot Embedding Adaptation with Transformer (FEAT)

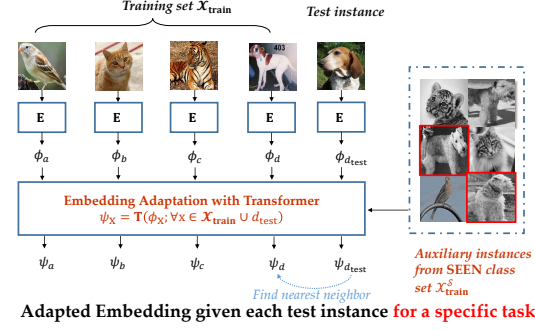


**Figure 2:** Illustration of our proposed Few-Shot Embedding Adaptation via Transformer (FEAT). Existing methods use the same embedding function  $\mathbf{E}$  for all tasks. In our approach, the embeddings are adapted to each target few-shot learning task. Instances from SEEN classes are also introduced to incorporate their relevance to the target unseen classes.

**Generalized FSL.** While prior works have assumed the test instances coming from unseen classes only, the generalized FSL setting considers test instances from both seen and unseen classes [7, 13, 34, 46]. In other words, although instances in  $\mathcal{D}_{\text{train}}$  all come from  $\mathcal{U}$ , the test instance may come from  $\mathcal{S} \cup \mathcal{U}$  and  $f(\mathbf{x}_{\text{test}}; \mathcal{D}_{\text{train}}) \rightarrow \{0, 1\}^{N+|\mathcal{S}|}$ .

### 4. Adapt Embedding for Few-shot Learning

In what follows, we describe our approach for few-shot learning (FSL). We start by describing the main idea (illustrative example in Figure 2), followed by several extensions.

#### 4.1. Main Idea

**Learning embeddings.** Our approach is based on the popular framework of learning embeddings for FSL [39, 44]. In particular, in the notion introduced in the previous section, the classifier  $f(\cdot)$  is composed of two elements. The first is an embedding function  $\phi_{\mathbf{x}} = \mathbf{E}(\mathbf{x}) \in \mathbb{R}^d$  that maps an instance  $\mathbf{x}$  to a representation space. The second component is to apply the nearest neighbor classifiers in this space. Note that only the embedding function is learned by optimizing the loss in Eq. 1. For reasons to be made clear in below, we refer this embedding function as *task-agnostic*.

**Adaptive embedding.** The key difference between our approach and the traditional ones is to learn *task-specific* embeddings. While the embedding  $\phi_{\mathbf{x}}$  is applied to any target task, we argue that it is not ideal. In particular, the embeddings do not necessarily highlight the most discriminative representation desired for a specific target task.

To this end, we introduce an adaption step where the embedding function  $\phi_{\mathbf{x}}$  (more precisely, its values on instances) is transformed. This transformation is a set-to-set

---

**Algorithm 1** Training strategy of embedding adaptation

---

**Require:** Seen class set  $\mathcal{S}$

- 1: **for all** iteration = 1,...,MaxIteration **do**
- 2:   Sample  $N$ -way  $M$ -shot  $(\mathcal{D}_{\text{train}}^{\mathcal{S}}, \mathcal{D}_{\text{test}}^{\mathcal{S}})$  from  $\mathcal{S}$
- 3:   Compute  $\phi_{\mathbf{x}} = \mathbf{E}(\mathbf{x})$ , for  $\mathbf{x} \in \mathcal{X}_{\text{train}}^{\mathcal{S}} \cup \mathcal{X}_{\text{test}}^{\mathcal{S}}$
- 4:   **for all**  $(\mathbf{x}_{\text{test}}^{\mathcal{S}}, \mathbf{y}_{\text{test}}^{\mathcal{S}}) \in \mathcal{D}_{\text{test}}^{\mathcal{S}}$  **do**
- 5:     Compute  $\{\psi_{\mathbf{x}} ; \forall \mathbf{x} \in \mathcal{X}_{\text{train}}^{\mathcal{S}} \cup \mathcal{X}_{\text{test}}^{\mathcal{S}}\}$  as Eq. 13
- 6:     Predict  $\hat{\mathbf{y}}_{\text{test}}^{\mathcal{S}}$  based on Eq. 3
- 7:     Compute  $\ell(\hat{\mathbf{y}}_{\text{test}}^{\mathcal{S}}, \mathbf{y}_{\text{test}}^{\mathcal{S}})$  as Eq. 1
- 8:   **end for**
- 9:   Compute  $\nabla_{\mathbf{E}, \mathbf{T}} \sum_{\mathbf{x}_{\text{test}}^{\mathcal{S}} \in \mathcal{X}_{\text{test}}^{\mathcal{S}}} \ell(\hat{\mathbf{y}}_{\text{test}}^{\mathcal{S}}, \mathbf{y}_{\text{test}}^{\mathcal{S}})$
- 10:   Update  $\mathbf{E}$  and  $\mathbf{T}$  with  $\nabla_{\mathbf{E}, \mathbf{T}}$  use SGD
- 11: **end for**
- 12: **return** Embedding function  $\mathbf{E}$  and set function  $\mathbf{T}$ .

---

function as the instances are bags, or sets without orders. Concretely, we aim to learn

$$\{\psi_{\mathbf{x}} ; \forall \mathbf{x} \in \mathcal{X}_{\text{train}} \cup \mathcal{X}_{\text{test}}\} = \mathbf{T}(\{\phi_{\mathbf{x}} ; \forall \mathbf{x} \in \mathcal{X}_{\text{train}} \cup \mathcal{X}_{\text{test}}\}) \quad (2)$$

where  $\mathcal{X}_{\text{train}}$  is a set of all the instances in the training set  $\mathcal{D}_{\text{train}}$  for the target task.

With adapted embedding  $\psi_{\mathbf{x}}$ , the test instance  $\mathbf{x}_{\text{test}}$  can be classified by computing nearest neighbors w.r.t.  $\mathcal{D}_{\text{train}}$ :

$$\begin{aligned} \hat{\mathbf{y}}_{\text{test}} &= f(\psi_{\mathbf{x}_{\text{test}}} ; \{\psi_{\mathbf{x}}, \forall (\mathbf{x}, \mathbf{y}) \in \mathcal{D}_{\text{train}}\}) \\ &\propto \exp(\mathbf{sim}(\psi_{\mathbf{x}_{\text{test}}}, \psi_{\mathbf{x}})) \cdot \mathbf{y}, \forall (\mathbf{x}, \mathbf{y}) \in \mathcal{D}_{\text{train}} \end{aligned} \quad (3)$$

Our approach is generally applicable to different types of task-agnostic embedding function  $\mathbf{E}$  and similarity measure  $\mathbf{sim}(\cdot, \cdot)$ , e.g., the (normalized) cosine similarity used in matching network [44] (MatchNet) or the negative distance used in prototypical network [39] (ProtoNet).

Both the embedding function  $\mathbf{E}$  and the set transformation function  $\mathbf{T}$  are optimized over synthesized few-shot learning tasks sampled from  $\mathcal{D}^{\mathcal{S}}$ , sketched in Alg. 1. Please note the key difference from conventional embedding-based FSL methods in *line 4 to line 8* where the embeddings are transformed.

## 4.2. Adaptation via Transformer

In this section, we describe in details about our **Few-Shot Embedding Adaptation via Transformer (FEAT)** approach, specifically how the set transformation function  $\mathbf{T}$  is implemented and optimized.

**Transformer.** We use the Transformer architecture [43] to implement  $\mathbf{T}$ . In particular, we employ self-attention mechanism [25, 43] to improve each instance embedding with consideration to its contextual embeddings.

Transformer is a store of triplets in the form of (query, key and value). It computes what is the right value for a query point — the query is first matched against a list of keys where each key has a value. The final value is then returned as the sum of all the values *weighted* by the proximity of the key to the query point. In our implementation, the query point is an instance whose embeddings we would like to find. The keys are a set of instances whose embeddings are already known and are encoded in the values. Specifically, following the original definitions in [43],  $\mathcal{Q}$  denotes the set of query points with  $\mathcal{K}$  for keys and  $\mathcal{V}$  for values — we describe later how we define them.

To compute proximity and return values, those points are first linearly mapped into some space:

$$\begin{aligned} Q &= W_Q^{\top} [\phi_{\mathbf{x}_q} ; \forall \mathbf{x}_q \in \mathcal{Q}] \in \mathbb{R}^{d \times |\mathcal{Q}|} \\ K &= W_K^{\top} [\phi_{\mathbf{x}_k} ; \forall \mathbf{x}_k \in \mathcal{K}] \in \mathbb{R}^{d \times |\mathcal{K}|} \\ V &= W_V^{\top} [\phi_{\mathbf{x}_v} ; \forall \mathbf{x}_v \in \mathcal{V}] \in \mathbb{R}^{d \times |\mathcal{V}|} \end{aligned} \quad (4)$$

A query point  $\mathbf{x}_q \in \mathcal{Q}$ 's similarity to the keys  $\mathcal{K}$  is then computed as “attention”:

$$\alpha_{qk} \propto \exp\left(\frac{\phi_{\mathbf{x}_q}^{\top} W_Q \cdot K}{\sqrt{d}}\right)$$

These attentions are then used as weights (after normalized to sum to 1) to compute the final embedding for  $\mathbf{x}_q$ :

$$\psi_{\mathbf{x}_q} = \phi_{\mathbf{x}_q} + \sum_k \alpha_{qk} V_{:,k} \quad (5)$$

$V_{:,k}$  is the  $k$ -th column of  $V$ . We defer more detailed description of this transformation to the implementation details (Section 5).

**Choice of the sets of keys and values.** In the standard FSL setup, the query instances ( $\mathcal{Q}$ ) are the union of the training and test instances of a target task, i.e.,

$$\mathcal{Q} = \mathcal{X}_{\text{train}} \cup \mathcal{X}_{\text{test}} \quad (6)$$

Additionally, we set  $\mathcal{K} = \mathcal{V} = \mathcal{Q}$ . Note that each of them has a different projection matrix. We refer this as FEAT.

We have also considered incorporating the instances from the SEEN classes to exploit their relation to the test instance in the UNSEEN classes:

$$\mathcal{K} = \mathcal{V} = \mathcal{X}_{\text{train}} \cup \mathcal{X}_{\text{test}} \cup \mathcal{X}_{\text{train}}^{\mathcal{S}}, \quad (7)$$

Note that  $\mathcal{Q}$  is unchanged for this setup, which we refer as FEAT<sup>+</sup>. Using the entire SEEN class training set  $\mathcal{X}_{\text{train}}^{\mathcal{S}}$  is computationally expensive, we approximate this procedure by performing a uniform sampling over all classes in  $\mathcal{S}$ . We refer the set of these sampled instances as auxiliary set since

they do not appear in the  $Q$  set. We explain the details about constructing such set in Section 5.

Likewise, for transductive FSL and generalized FSL, we construct different sets of  $\mathcal{K}$  and  $\mathcal{V}$ . Details are in the supplementary material.

**Contrastive attention learning (CAL).** To learn the linear mapping  $W_Q, W_K$  and  $W_V$  for the Transformer architecture, we leverage the contrastive loss that the two instances should be mapped close to each other if they are from the same class. For  $\mathbf{x}_q$  and  $\mathbf{x}_k$  being mapped close to each other, the attention coefficients  $\alpha_{qk'}$  should peak at the  $k' = k$ . Viewing the attention coefficients as a vector of probabilities, we thus reduce its KL divergence from the “ideal” proximity vector which is a binary vector having one at  $k$ th location. We add this term to the loss function

$$\begin{aligned} \mathcal{L}(\hat{\mathbf{y}}_{\text{test}}, \mathbf{y}_{\text{test}}) &= \ell(\hat{\mathbf{y}}_{\text{test}}, \mathbf{y}_{\text{test}}) \\ &+ \lambda \sum_{\mathbf{x}_q \in \mathcal{Q}} \sum_{\mathbf{y}_k = \mathbf{y}_q} \alpha_{qk} \log \alpha_{qk} \end{aligned} \quad (8)$$

For details, please see the supplementary material.

## 5. Experimental Setups

**Datasets.** The *MiniImageNet* dataset [44] is a subset of the ImageNet [36] that includes a total number of 100 classes and 600 examples per class. We follow the setup provided by [33], and use 64 classes as SEEN categories, 16 and 20 as two sets of UNSEEN categories for model validation and evaluation respectively. In addition to this, we also use the Caltech-UCSD Birds (CUB) 200-2011 dataset [45], which is initially designed for fine-grained classification. It contains in total 11,788 images of birds over 200 species. On CUB, we randomly sampled 100 species as SEEN classes, another two 50 species are used as two UNSEEN sets [42]. Please refer to supplementary material for more details.

**Evaluation protocols.** Previous approaches [10, 39, 42] usually follow the original setting of [44] and evaluate the models on 600 sampled target tasks (15 test instances per class). In a later study [37], it was suggested that such evaluation process can potentially introduce high variances. Therefore, we follow the new and more trustworthy evaluation setting [37] to evaluate both baseline models and our approach on 10,000 sampled tasks. We report the mean accuracy (in %) as well as the 95% confidence interval.

**Baselines.** We re-implement two important methods — matching network [44] (**MatchNet**) and prototypical network [39] (**ProtoNet**) respectfully. There are key differences. First, we found it is very important to add a scalar

temperature to scale the logits of both approaches, which is consistent with observations in [30]. Secondly, we apply an additional pre-training stage to the backbone neural networks and use it as an initialization for both approaches. We find such pre-training on the SEEN classes of each dataset is effective and can significantly accelerate the time until convergence for each method. Such pre-training is applied to both baselines and our approaches.

Besides these two methods, a straightforward baseline to our proposed embedding adaptation framework uses a recurrent model (**BILSTM**) to approximating the set function  $\mathbf{T}$ . This is similar to the fully conditional embedding in [44]. Note that such instantiation of the set function  $\mathbf{T}$  can be directly learned in our learning framework (except CAL is not applicable in this case). Therefore, same as our proposed approach, two variants BILSTM(**MatchNet**) and BILSTM(**ProtoNet**) can be directly obtained. We compare our **FEAT (MatchNet)** and **FEAT (ProtoNet)** directly to these two baselines to demonstrate the effectiveness of using a permutation-invariant set function instead of a sequence model. Please see supplementary for details.

**Implementation details.** We consider two backbone convolutional networks as suggested in literature. 1) A four-layer convolution network (ConvNet) [39, 42, 44] and 2) A wide residual network (ResNet) [30, 32, 37], as instance embedding functions  $\mathbf{E}$  to the purpose of fair comparisons. As mentioned before, we applied an additional pre-training strategy as suggested in [32, 37]. We refer readers to supplementary material for further details. We follow the architecture as presented in [43] to build our **FEAT** and **FEAT<sup>+</sup>** models. The hidden dimensions for the linear transformations in our **FEAT** models is set to be 64 for ConvNet and 640 for ResNet. We empirically observed that the shallow transformer (with one set of projection and one stacked layer) gives the best overall performance (also studied in Section 6.2). For **FEAT<sup>+</sup>**, we construct auxiliary set from  $\mathcal{X}_{\text{train}}^S$  by sampling 2 instances from each class in  $\mathcal{S}$ . During the training, stochastic gradient descent with Adam [16] optimizer is employed, with the initial learning rate set to be 1e-3. As the backbone network has been pre-trained, we scale the learning rate for those set of parameters by 0.1. To the purpose of reproducibility, our implementation is made publicly available at <https://github.com/Sha-Lab/FEAT>.

## 6. Standard Few-Shot Classification

We evaluate our proposed **FEAT** from various perspectives, on two widely used few-shot learning datasets — *MiniImageNet* [44] and CUB [45]. We first compare our proposed method with our baselines as well as previous methods on the benchmark dataset and then perform detailed analysis on the ablated models.

**Table 1:** Few-shot classification accuracy on *MiniImageNet*. Our implementation methods are measured over 10,000 test trials. We remove the 95% confidence interval in this table for simplicity. Please refer to supplementary material for complete details.

Setups →	1-Shot 5-Way		5-Shot 5-Way	
Backbone Network →	ConvNet	ResNet	ConvNet	ResNet
MatchNet [44]	43.40	-	51.09	-
MAML [10]	48.70	-	63.11	-
ProtoNet [39]	49.42	-	68.20	-
RelationNet [41]	51.38	-	67.07	-
PFA [32]	54.53	59.60	67.87	73.74
TADAM [30]	-	58.50	-	76.70
LEO [37]	-	61.76	-	77.59
<b>Baselines</b>				
MatchNet	52.87	60.66	67.49	75.05
ProtoNet	52.61	61.40	71.33	76.56
BILSTM(MatchNet)	54.59	59.36	68.20	72.98
BILSTM(ProtoNet)	54.10	55.73	69.39	69.93
<b>Our approach</b>				
FEAT (MatchNet)	55.15	60.08	70.49	77.87
FEAT (ProtoNet)	55.21	<b>62.60</b>	<b>72.17</b>	78.06
FEAT <sup>+</sup> (MatchNet)	55.33	60.92	69.68	76.35
FEAT <sup>+</sup> (ProtoNet)	<b>55.79</b>	61.72	71.79	<b>78.38</b>

**Table 2:** Few-shot classification performance with ConvNet backbone on CUB dataset (mean accuracy $\pm$ 95% confidence interval). Our implementation methods are measured over 10,000 test trials.

Setups →	1-Shot 5-Way		5-Shot 5-Way	
MatchNet [44]	$61.16 \pm 0.89$		$72.86 \pm 0.70$	
MAML [10]	$55.92 \pm 0.95$		$72.09 \pm 0.76$	
ProtoNet [39]	$51.31 \pm 0.91$		$70.77 \pm 0.69$	
RelationNet [41]	$62.45 \pm 0.98$		$76.11 \pm 0.69$	
<b>Baselines</b>				
MatchNet	$67.73 \pm 0.23$		$79.00 \pm 0.16$	
ProtoNet	$63.72 \pm 0.22$		$81.50 \pm 0.15$	
BILSTM(MatchNet)	$67.40 \pm 0.23$		$78.56 \pm 0.17$	
BILSTM(ProtoNet)	$66.98 \pm 0.23$		$80.08 \pm 0.16$	
<b>Our approach</b>				
FEAT (MatchNet)	$68.44 \pm 0.22$		$80.78 \pm 0.16$	
FEAT (ProtoNet)	$68.65 \pm 0.22$		<b><math>83.03 \pm 0.15</math></b>	
FEAT <sup>+</sup> (MatchNet)	<b><math>68.96 \pm 0.22</math></b>		$81.33 \pm 0.16$	
FEAT <sup>+</sup> (ProtoNet)	$68.35 \pm 0.22$		$82.69 \pm 0.15$	

## 6.1. Main Results

Results on *MiniImageNet* (Table 8) and CUB (Table 2) show FEAT and FEAT<sup>+</sup> outperform our baselines and previous state-of-the-art methods, which validates the effectiveness of our method for few-shot classification.

The comparisons with more recent works such as

PFA [32], LEO [37], and TADAM [30] are fair since all these methods either use the pre-trained weights to initialize their models or include a classification objective that is similar to the ones used in pre-training stage. With the same training strategy applied, our re-implemented MatchNet and ProtoNet achieve better results than their previously reported ones. Note that ProtoNet works well especially on the 5-shot learning scenario, which is consistent with previous observations [32, 39, 41]. In our baseline that uses BILSTM to implement the set transformation  $\mathbf{T}$ , it improves the ability of input embedding on ConvNet and especially the 1-shot learning case. We empirically find that the way regarding embedding set as a sequence becomes unstable and difficult to train when either the number of elements in the set increases or the backbone network becomes more complicated. In the contrast, we found that transformer can better instantiate the set-to-set function, with stable and more consistent improvement in all learning cases. It demonstrates that it is important to use a set-to-set function, which is intrinsically permutation invariant. The extension FEAT<sup>+</sup> with auxiliary sampled instances can get a slightly better accuracy than the vanilla FEAT, but the helpful of the auxiliary set cannot always be discovered with more training examples. We observe the sampled auxiliary set makes the results of FEAT<sup>+</sup> have a large variance when evaluating with limited trials. For example, in the classical protocol on 600 sampled tasks, FEAT<sup>+</sup> (ProtoNet) (with the ConvNet) can achieve 57.15% for 1-shot learning performance, with a good random seed (also it can reach 54.35% with a bad seed). Evaluating all approaches with 10,000 sampled tasks can produce more trustworthy results.

In addition, we show our proposed approach can consistently improve the task-agnostic embedding for different datasets <sup>1</sup>. Comparing with our re-implemented baselines and previous results, FEAT and FEAT<sup>+</sup> achieve better performances.

## 6.2. Ablation Studies

In this section, we perform further analysis for our proposed FEAT and its ablated variant based on ProtoNet, on the *MiniImageNet* dataset, using the ConvNet as the backbone network.

**Is FEAT improving task-agnostic embeddings?** As a first step to this ablation study, we perform sanity check to verify whether our proposed method is really improving the task-agnostic embedding  $\mathbf{E}$  or not. To do so, we surgery our model and evaluate the learnt instance embedding function  $\mathbf{E}$  through directly measure its few-shot classification performance. As a result, we found that this task-agnostic embedding can only achieve 51.72% and 70.83% on 1-shot

<sup>1</sup>Results of previous methods are cited from [3].

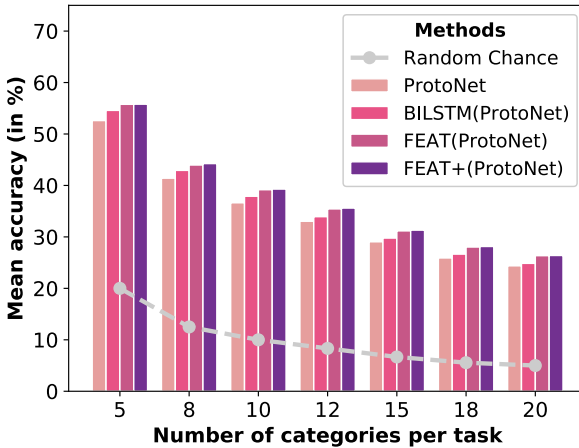


**Figure 3:** One-shot learning accuracy when evaluated on more unseen tasks with larger number of classes ( $N=\{5, 8, 10, 12, 15, 18, 20\}$ ). Models are only trained for 5-way classification tasks.

and 5-shot tasks respectively, whilst its counter part (FEAT(ProtoNet)) achieves 55.21% and 72.17%. This verifies our main claim of the effectiveness in embedding adaptation.

#### Can FEAT generalize to more classes in the target tasks?

We evaluate the effectiveness of the learned few-shot model when applying to tasks with more classes. After learning models with 1-shot 5-way tasks, we test ProtoNet, BILSTM(ProtoNet), and our FEAT variants on one-shot learning tasks with  $N = \{5, 8, 12, 15, 18, 20\}$ . Results are shown in the Figure. 6. Because the classification problem becomes more difficult with more classes involved (as the random chance of success decreases), the evaluation accuracies of all methods decrease. However, we observe that BILSTM fail to extrapolate as good as our FEAT variants. As the relative performance gain over vanilla ProtoNet from BILSTM deceases towards almost zero. In the contrast, our FEAT and FEAT<sup>+</sup> can still attain relatively superior performances gain in this case. Such extrapolation capability might largely due to the fact that Transformer is a set-to-set function.

**The effectiveness of CAL.** The contrastive attention learning incorporates the label information of each instance for the attention learning in transformer. We empirically find the addition of CAL can help prevent overfitting and makes the optimization more stable. The results with ( $\lambda = 10$ ) and without ( $\lambda = 0$ ) the regularizer are in Table 10, where using the CAL gets higher test accuracies. Please see supplementary material for complete ablation study of different  $\lambda$ .

**Will deeper and multi-head transformer help?** In our current implementation of the set-to-set transformation

**Table 3:** Ablation studies on effects of regularization.

Setups →	1-Shot 5-Way	5-Shot 5-Way
$\lambda = 0.0$		
FEAT(ProtoNet)	$54.65 \pm 0.20$	$71.47 \pm 0.16$
FEAT <sup>+</sup> (ProtoNet)	$55.39 \pm 0.11$	$70.99 \pm 0.16$
$\lambda = 10.0$		
FEAT(ProtoNet)	$55.21 \pm 0.20$	$72.17 \pm 0.16$
FEAT <sup>+</sup> (ProtoNet)	$55.79 \pm 0.11$	$71.79 \pm 0.16$

**Table 4:** Ablation studies on the number of heads in transformer (used by FEAT (ProtoNet)). The models are evaluated on *MiniImageNet*, with ConvNet as backbone. Mean accuracy (in %) is reported.

# of heads	1-Shot 5-Way	5-Shot 5-Way
1	$55.21 \pm 0.20$	$72.17 \pm 0.16$
2	$55.14 \pm 0.20$	$71.51 \pm 0.16$
4	$55.04 \pm 0.20$	$71.57 \pm 0.16$
8	$54.42 \pm 0.20$	$71.21 \pm 0.16$

**Table 5:** Ablation studies on *MiniImageNet*, to the number of stacked layers in transformer (used by FEAT (ProtoNet)), with ConvNet.

# of layers	1-Shot 5-Way	5-Shot 5-Way
1	$55.77 \pm 0.20$	$72.17 \pm 0.16$
2	$55.08 \pm 0.20$	$71.14 \pm 0.16$
3	$54.93 \pm 0.20$	$70.79 \pm 0.16$

function  $T$ , we make use of shallow and simple transformer, i.e., one layer and one head (set of projection). From [43], the transformer can be equipped with complex components using multiple heads and deep stacked layers. We evaluate this augmented structure, with attention heads increases to 2,4,8, as well as with number of layers increases to 2 and 3. As in Table 4 and Table 5, we empirically observe that more complicated structures do not result in improved performance. We find that with more layers of transformer stacked, the difficulty of optimization increases and it becomes harder to train models until their convergence. Whilst for models with more heads, the models seem to over-fit heavily on the training data, even with the usage of CAL. It might require some careful regularization to prevent over-fitting, which we leave for future work.

### 6.3. Qualitative Visualization of Attention

Recall that FEAT<sup>+</sup> adapt the embedding with the help of auxiliary instances from the seen class set  $\mathcal{S}$ . The attention between an test instance and auxiliary sampled seen class instances reveals inter-class similarity: the larger the value,

Training instance	Hunting dog	Ant	Hourglass	Mixing bowl	Trifle
Test instance					
Hunting dog	Newfoundland dog 	Tibetan mastiff 	Komondor 	Gordon setter 	Miniature poodle 
Trifle	0.1242 	0.0971 	0.0609 	0.0558 	0.0386 
	0.1029	0.0855	0.0781	0.0370	0.0333
Training instance	Electric guitar	Scoreboard	Mixing bowl	Dalmatian	Bookshop
Test instance					
Bookshop	Tobacco shop 	Prayer rug 	Tobacco shop 	Carousel 	Slot 
Dalmatian	0.1343 	0.0834 	0.0389 	0.0558 	0.0385 
	0.1365	0.0801	0.0612	0.0462	0.0340

**Figure 4:** The embedding adaptation facilitated instances selected by FEAT<sup>+</sup> in two tasks (related instances come first). Texts above/below images are the labels and the value of attention.

**Table 6:** Results of models for transductive FSL with ConvNet backbone on *MiniImageNet*.

Setups →	1-Shot 5-Way	5-Shot 5-Way
<b>Standard</b>		
ProtoNet	52.61 ± 0.20	71.33 ± 0.16
FEAT (ProtoNet)	55.21 ± 0.20	72.17 ± 0.16
<b>Transductive</b>		
Semi-ProtoNet [35]	50.41 ± 0.31	64.39 ± 0.24
TPN [26]	54.72 ± 0.84	69.25 ± 0.67
FEAT(ProtoNet)	<b>56.49 ± 0.21</b>	<b>72.65 ± 0.16</b>
FEAT <sup>+</sup> (ProtoNet)	55.40 ± 0.20	70.16 ± 0.67

the more important the auxiliary instance help to adapt the test instance embedding. For a test image, we sort the different-class auxiliary instances based on the descending attention values. Results of four test cases in two 1-shot tasks are shown in Figure 7. We find that the auxiliary set helps especially when the training instances of a task does not have high discriminative-ability.

## 7. Extended Few-Shot Classification

**Transductive FSL.** We list the result of transductive few-shot classification in Table 12, where the unlabeled test instances arrive simultaneously when classifying a test in-

**Table 7:** Results of generalized FEAT variants with ConvNet backbone on *MiniImageNet*. All methods are evaluated on instances composed by SEEN classes, UNSEEN classes, and both of them (JOINT), respectively.

Measures →	SEEN	UNSEEN	JOINT
ProtoNet	41.73 ± 0.03	48.64 ± 0.20	35.69 ± 0.03
FEAT(ProtoNet)	43.94 ± 0.03	<b>49.72 ± 0.20</b>	40.50 ± 0.03
FEAT <sup>+</sup> (ProtoNet)	<b>47.28 ± 0.03</b>	48.08 ± 0.19	<b>43.50 ± 0.03</b>
Random Chance	1.56	20.00	1.45

stance. We compare with two previous approaches, Semi-ProtoNet [35] and TPN [26]. In this setting, our model leverage the unlabeled test instances to augment the transformer as discussed in Sec. 4.2, and the embedding adaptation takes relationship of all test instances into consideration. From the results, FEAT achieves further performance improvement compared with standard setting. The performance gain induced by the transductive FEAT (ProtoNet) is more significant in the one-shot learning setting comparing to the five-shot scenario. Please find more discussions in the supplementary material.

**Generalized FSL.** In this scenario [7, 12, 13, 46], we care not only about classifying test instances from a  $N$ -way  $M$ -shot task sampled on UNSEEN set, but also test instances from existing classes in SEEN set. Since classes on SEEN set are also required for evaluation, we hold out 150 instances from each of the 64 seen classes for model validation and evaluation in *MiniImageNet*. Next, given a 1-shot 5-way training set  $\mathcal{D}_{\text{train}}$ , we consider three evaluation protocols based on different evaluation sets: UNSEEN measures the mean classification accuracy on test instances only from UNSEEN set (5-Way few-shot classification); SEEN measures the mean accuracy on test instances only from SEEN set (64-Way classification); JOINT measures the mean accuracy on test instances from both SEEN and UNSEEN sets (69-Way mixed classification). Based on the strategy of [7, 46], we tune the prior of seen/unseen class probabilities with a constant bias over the validation set as calibration value, which enable all models to directly make generalized predictions (via subtracting this calibration factor from seen class’s prediction score).

The results can be found in Table 13. The superiority of FEAT is maintained in this setting. The FEAT<sup>+</sup> gets better performance especially in the JOINT evaluation, which verifies its ability to handle both seen and novel few-shot classifications. Please find more details in the supplementary.

## 8. Discussion

A common embedding space fails to tailor discriminative visual knowledge for a target task especially when there are a few labeled training data. We propose to do Few-shot Embedding Adaptation with Transformer (FEAT), which customizes a task-specific embedding spaces via a self-attention architecture. The adapted embedding spaces leverage both the relationship between target task instances and the relationship with SEEN classes, which leads to discriminative instance representations. FEAT demonstrates the state-of-the-art performance on *MiniImageNet* and *CUB* datasets, and its superiority can generalize to transductive as well as generalized few-shot classifications. Extension of FEAT with multiple modalities could be future work.

**Acknowledgments** We appreciate Liyu Chen, Bowen Zhang for their constructive feedbacks to an earlier version of this paper. This work is partially supported by DARPA# FA8750-18-2-0117, NSF IIS-1065243, 1451412, 1513966/1632803/1833137, 1208500, CCF-1139148, a Google Research Award, an Alfred P. Sloan Research Fellowship, gifts from Facebook and Netflix, ARO# W911NF-12-1-0241 and W911NF-15-1-0484, and China Scholarship Council.

## References

- [1] Z. Akata, F. Perronnin, Z. Harchaoui, and C. Schmid. Label-embedding for attribute-based classification. In *2013 IEEE Conference on Computer Vision and Pattern Recognition*, pages 819–826. IEEE, 2013. [2](#)
- [2] M. Andrychowicz, M. Denil, S. G. Colmenarejo, M. W. Hoffman, D. Pfau, T. Schaul, and N. de Freitas. Learning to learn by gradient descent by gradient descent. In *Advances in Neural Information Processing Systems 29*, pages 3981–3989. Curran Associates, Inc., 2016. [2](#)
- [3] Anonymous. A closer look at few-shot classification. In *Submitted to International Conference on Learning Representations*, 2019. under review. [6](#)
- [4] L. J. Ba, R. Kiros, and G. E. Hinton. Layer normalization. *CoRR*, abs/1607.06450, 2016. [12](#)
- [5] S. Changpinyo, W.-L. Chao, B. Gong, and F. Sha. Synthesized classifiers for zero-shot learning. In *Proceedings of the IEEE Conference on Computer Vision and Pattern Recognition*, pages 5327–5336, 2016. [2](#)
- [6] S. Changpinyo, W.-L. Chao, and F. Sha. Predicting visual exemplars of unseen classes for zero-shot learning. In *2017 IEEE International Conference on Computer Vision (ICCV)*, pages 3496–3505. IEEE, 2017. [2](#)
- [7] W.-L. Chao, S. Changpinyo, B. Gong, and F. Sha. An empirical study and analysis of generalized zero-shot learning for object recognition in the wild. In *Proceedings of the 14th European Conference on Computer Vision*, pages 52–68, Amsterdam, The Netherlands, 2016. [3, 8](#)
- [8] M. Dehghani, S. Gouws, O. Vinyals, J. Uszkoreit, and L. Kaiser. Universal transformers. *CoRR*, abs/1807.03819, 2018. [14](#)
- [9] J. Deng, W. Dong, R. Socher, L.-J. Li, K. Li, and L. Fei-Fei. Imagenet: A large-scale hierarchical image database. In *Computer Vision and Pattern Recognition, 2009. CVPR 2009. IEEE Conference on*, pages 248–255. Ieee, 2009. [1](#)
- [10] C. Finn, P. Abbeel, and S. Levine. Model-agnostic meta-learning for fast adaptation of deep networks. In *Proceedings of the 34th International Conference on Machine Learning*, pages 1126–1135, Sydney, Australia, 2017. [1, 2, 3, 5, 6, 14, 15](#)
- [11] V. Garcia and J. Bruna. Few-shot learning with graph neural networks. *CoRR*, abs/1711.04043, 2017. [2](#)
- [12] S. Gidaris and N. Komodakis. Dynamic few-shot visual learning without forgetting. In *Proceedings of the IEEE Conference on Computer Vision and Pattern Recognition*, pages 4367–4375, Salt Lake City, UT, 2018. [8](#)
- [13] B. Hariharan and R. B. Girshick. Low-shot visual recognition by shrinking and hallucinating features. In *IEEE International Conference on Computer Vision*, pages 3037–3046, Venice, Italy, 2017. [3, 8](#)
- [14] K. He, X. Zhang, S. Ren, and J. Sun. Deep residual learning for image recognition. In *Proceedings of the IEEE conference on computer vision and pattern recognition*, pages 770–778, 2016. [1](#)
- [15] S. Ioffe and C. Szegedy. Batch normalization: Accelerating deep network training by reducing internal covariate shift. In *Proceedings of the 32nd International Conference on Machine Learning*, pages 448–456, Lille, France, 2015. [13](#)
- [16] D. P. Kingma and J. Ba. Adam: A method for stochastic optimization. *CoRR*, abs/1412.6980, 2014. [5, 14](#)
- [17] T. N. Kipf and M. Welling. Semi-supervised classification with graph convolutional networks. *CoRR*, abs/1609.02907, 2016. [2](#)
- [18] G. Koch, R. Zemel, and R. Salakhutdinov. Siamese neural networks for one-shot image recognition. In *ICML Deep Learning Workshop*, volume 2, 2015. [2](#)
- [19] A. Krizhevsky, I. Sutskever, and G. E. Hinton. Imagenet classification with deep convolutional neural networks. In *Advances in neural information processing systems*, pages 1097–1105, 2012. [1](#)
- [20] B. M. Lake, R. Salakhutdinov, J. Gross, and J. B. Tenenbaum. One shot learning of simple visual concepts. In *Proceedings of the 33th Annual Meeting of the Cognitive Science Society*, Boston, MA, 2011. [1](#)
- [21] B. M. Lake, R. Salakhutdinov, and J. B. Tenenbaum. Human-level concept learning through probabilistic program induction. *Science*, 350(6266):1332–1338, 2015. [1](#)
- [22] C. H. Lampert, H. Nickisch, and S. Harmeling. Attribute-based classification for zero-shot visual object categorization. *IEEE Transactions on Pattern Analysis and Machine Intelligence*, 36(3):453–465, 2014. [2](#)
- [23] Y. Lee and S. Choi. Gradient-based meta-learning with learned layerwise metric and subspace. In *Proceedings of the 35th International Conference on Machine Learning*, pages 2933–2942, Stockholm, Sweden, 2018. [2](#)
- [24] F. Li, R. Fergus, and P. Perona. One-shot learning of object categories. *IEEE Transactions on Pattern Analysis and Machine Intelligence*, 28(4):594–611, 2006. [1](#)
- [25] Z. Lin, M. Feng, C. N. dos Santos, M. Yu, B. Xiang, B. Zhou, and Y. Bengio. A structured self-attentive sentence embed-

ding. In *ICLR*, 2017. 2, 4

[26] Y. Liu, J. Lee, M. Park, S. Kim, and Y. Yang. Transductive propagation network for few-shot learning. *CoRR*, abs/1805.10002, 2018. 3, 8, 16

[27] D. Mahajan, R. Girshick, V. Ramanathan, K. He, M. Paluri, Y. Li, A. Bharambe, and L. van der Maaten. Exploring the limits of weakly supervised pretraining. *ECCV*, 2018. 1

[28] L. Metz, N. Maheswaranathan, B. Cheung, and J. Sohl-Dickstein. Learning unsupervised learning rules. *CoRR*, abs/1804.00222, 2018. 2

[29] A. Nichol, J. Achiam, and J. Schulman. On first-order meta-learning algorithms. *CoRR*, abs/1803.02999, 2018. 2

[30] B. N. Oreshkin, P. Rodríguez, and A. Lacoste. TADAM: task dependent adaptive metric for improved few-shot learning. *CoRR*, abs/1805.10123, 2018. 5, 6, 11, 13, 15

[31] N. Parmar, A. Vaswani, J. Uszkoreit, L. Kaiser, N. Shazeer, A. Ku, and D. Tran. Image transformer. In *Proceedings of the 35th International Conference on Machine Learning*, pages 4052–4061, Stockholm, Sweden, 2018. 2

[32] S. Qiao, C. Liu, W. Shen, and A. L. Yuille. Few-shot image recognition by predicting parameters from activations. *CoRR*, abs/1706.03466, 2017. 2, 5, 6, 13, 14, 15, 16

[33] S. Ravi and H. Larochelle. Optimization as a model for few-shot learning. In *In International Conference on Learning Representations*, 2017. 2, 5

[34] M. Ren, R. Liao, E. Fetaya, and R. S. Zemel. Incremental few-shot learning with attention attractor networks. *CoRR*, abs/1810.07218, 2018. 3

[35] M. Ren, E. Triantafillou, S. Ravi, J. Snell, K. Swersky, J. B. Tenenbaum, H. Larochelle, and R. S. Zemel. Meta-learning for semi-supervised few-shot classification. *CoRR*, abs/1803.00676, 2018. 3, 8, 16

[36] O. Russakovsky, J. Deng, H. Su, J. Krause, S. Satheesh, S. Ma, Z. Huang, A. Karpathy, A. Khosla, M. S. Bernstein, A. C. Berg, and F. Li. Imagenet large scale visual recognition challenge. *International Journal of Computer Vision*, 115(3):211–252, 2015. 5

[37] A. A. Rusu, D. Rao, J. Sygnowski, O. Vinyals, R. Pascanu, S. Osindero, and R. Hadsell. Meta-learning with latent embedding optimization. *CoRR*, abs/1807.05960, 2018. 1, 2, 5, 6, 13, 14, 15, 16

[38] K. Simonyan and A. Zisserman. Very deep convolutional networks for large-scale image recognition. *arXiv preprint arXiv:1409.1556*, 2014. 1

[39] J. Snell, K. Swersky, and R. S. Zemel. Prototypical networks for few-shot learning. In *Advances in Neural Information Processing Systems 30*, pages 4080–4090. Curran Associates, Inc., 2017. 1, 2, 3, 4, 5, 6, 11, 13, 15

[40] N. Srivastava, G. E. Hinton, A. Krizhevsky, I. Sutskever, and R. Salakhutdinov. Dropout: a simple way to prevent neural networks from overfitting. *Journal of Machine Learning Research*, 15(1):1929–1958, 2014. 12

[41] F. Sung, Y. Yang, L. Zhang, T. Xiang, P. H. S. Torr, and T. M. Hospedales. Learning to compare: Relation network for few-shot learning. *CoRR*, abs/1711.06025, 2017. 2, 6, 15

[42] E. Triantafillou, R. S. Zemel, and R. Urtasun. Few-shot learning through an information retrieval lens. In *Advances in Neural Information Processing Systems 30*, pages 2252–2262. Curran Associates, Inc., 2017. 1, 2, 5, 13

[43] A. Vaswani, N. Shazeer, N. Parmar, J. Uszkoreit, L. Jones, A. N. Gomez, L. Kaiser, and I. Polosukhin. Attention is all you need. In *Advances in Neural Information Processing Systems 30*, pages 6000–6010. Curran Associates, Inc., 2017. 2, 4, 5, 7, 12, 13

[44] O. Vinyals, C. Blundell, T. Lillicrap, K. Kavukcuoglu, and D. Wierstra. Matching networks for one shot learning. In *Advances in Neural Information Processing Systems 29*, pages 3630–3638. Curran Associates, Inc., 2016. 1, 2, 3, 4, 5, 6, 11, 13, 15

[45] C. Wah, S. Branson, P. Welinder, P. Perona, and S. Belongie. The Caltech-UCSD Birds-200-2011 Dataset. Technical Report CNS-TR-2011-001, California Institute of Technology, 2011. 5, 13

[46] Y. Wang, R. B. Girshick, M. Hebert, and B. Hariharan. Low-shot learning from imaginary data. In *Proceedings of the IEEE Conference on Computer Vision and Pattern Recognition*, pages 7278–7286, Salt Lake City, UT, 2018. 3, 8

[47] X.-S. Wei, P. Wang, L. Liu, C. Shen, and J. Wu. Piecewise classifier mappings: Learning fine-grained learners for novel categories with few examples. *CoRR*, abs/1805.04288, 2018. 2

[48] M. Zaheer, S. Kottur, S. Ravanbakhsh, B. Póczos, R. R. Salakhutdinov, and A. J. Smola. Deep sets. In *Advances in Neural Information Processing Systems 30*, pages 3394–3404. Curran Associates, Inc., 2017. 11, 14

[49] B. Zhou, A. Lapedriza, A. Khosla, A. Oliva, and A. Torralba. Places: A 10 million image database for scene recognition. *IEEE Transactions on Pattern Analysis and Machine Intelligence*, 2017. 1

## Supplementary Material

In this supplementary material, we discuss the omitted details in the main paper, with a outline as what follows:

- Details of baseline methods (cf. Section A).
- Details of the Transformer (cf. Section B).
- Details of implementation and experimental setups (cf. Section C.)
- Additional experimental results. (cf. Section D).

### A. Details of Baseline Methods

In this section, we will describe two important embedding learning baselines *i.e.* Matching Network (MatchNet) [44] and Prototypical Network (ProtoNet) [39], and an additional baseline with a simple form of set function.

**MatchNet and ProtoNet.** Both MatchNet and ProtoNet stress the learning of the embedding function  $\mathbf{E}$  from the source task data  $\mathcal{D}^S$  with a meta-learning routing similar to Alg. 1 in the main text.

Given the training data  $\mathcal{D}_{\text{train}} = \{\mathbf{x}_i, \mathbf{y}_i\}_{i=1}^{NM}$  of a target  $M$ -shot  $N$ -way classification task, we can obtain the embedding of each training instance based on the function  $\mathbf{E}$ :

$$\phi(\mathbf{x}_i) = \mathbf{E}(\mathbf{x}_i), \forall \mathbf{x}_i \in \mathcal{X}_{\text{train}} \quad (9)$$

To classify a test instance  $\mathbf{x}_{\text{test}}$ , we perform nearest neighbor classification, *i.e.*,

$$\begin{aligned} \hat{\mathbf{y}}_{\text{test}} &\propto \exp(\gamma \cos(\phi_{\mathbf{x}_{\text{test}}}, \phi_{\mathbf{x}_i})) \cdot \mathbf{y}_i \\ &= \frac{\exp(\gamma \cos(\phi_{\mathbf{x}_{\text{test}}}, \phi_{\mathbf{x}_i}))}{\sum_{\mathbf{x}_i \in \mathcal{X}_{\text{train}}} \exp(\gamma \cos(\phi_{\mathbf{x}_{\text{test}}}, \phi_{\mathbf{x}_i}))} \cdot \mathbf{y}_i \end{aligned} \quad (10)$$

where  $\forall (\mathbf{x}_i, \mathbf{y}_i) \in \mathcal{D}_{\text{train}}$

$\cos$  is the normalized cosine similarity.  $\gamma > 0$  is a temperature of a scalar value over the similarity score, which is found very important for the final performance [30]. During the experiments, we tune this value from  $\{0.1, 1, 16, 32, 64, 128\}$ . This similarity-based classification rule is used in the MatchNet.

The ProtoNet has two key differences comparing with MatchNet. First, when  $M > 1$  in the target task, ProtoNet uses only the class center (prototype) of each class to compute the nearest neighbor. Here a class center is the mean of the embeddings for all training instances. In addition, it uses negative distance rather than cosine similarity as the distance metric to find the nearest neighbor:

$$\mathbf{c}_n = \frac{1}{M} \sum_{\mathbf{x}_i \in \mathcal{X}_{\text{train}}} \phi(\mathbf{x}_i), \forall n = 1, \dots, N \quad (11)$$

$$\hat{\mathbf{y}}_{\text{test}} = \frac{\exp(-\gamma \|\phi_{\mathbf{x}_{\text{test}}} - \mathbf{c}_n\|_2^2)}{\sum_{n=1}^N \exp(-\gamma \|\phi_{\mathbf{x}_{\text{test}}} - \mathbf{c}_n\|_2^2)} \mathbf{y}_n \quad (12)$$

### Transformer in Detail

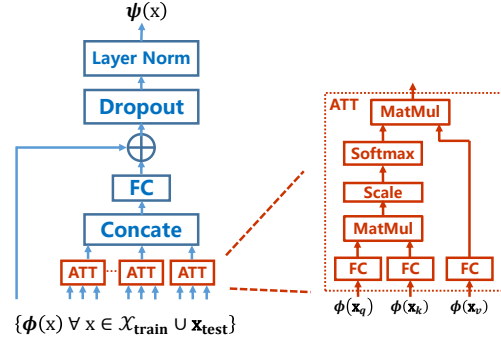


**Figure 5:** Illustration of structure of Transformer used in our proposed Few-Shot Embedding Adaptation via Transformer (FEAT). This plot shows the concrete operations a transformer adapt the embedding  $\phi(\mathbf{x})$  to  $\psi(\mathbf{x})$ . “ATT” is the attention block in the transformer.

Similar to the aforementioned scalar temperature for MatchNet, in Eq. 12 we also consider the scale  $\gamma$ . Here we abuse the notation by using  $\mathbf{y}_i = n$  to enumerate the instances with label  $n$ .

**Additional baseline with simple set function.** In the paper, we propose an embedding adaptation step ( $\phi(\mathbf{x}) \rightarrow \psi(\mathbf{x})$ ) to facilitate the few-shot classification, which is implemented by a set-to-set transformation  $\mathbf{T}$ :

$$\{\psi_{\mathbf{x}} ; \forall \mathbf{x} \in \mathcal{X}_{\text{train}} \cup \mathcal{X}_{\text{test}}\} = \mathbf{T}(\{\phi_{\mathbf{x}} ; \forall \mathbf{x} \in \mathcal{X}_{\text{train}} \cup \mathcal{X}_{\text{test}}\}) \quad (13)$$

The adapted embedding is influenced by the other instances in the sets. One main essential property of this function is the permutation-invariant “set” property, which suggests that items within a set can be ordered randomly.

Deep sets [48] suggests that for a generic aggregation function over a set, it should be the transformed sum of all elements in the set. Therefore, a very simple set-to-set transformation baseline besides the Transformer can be one that involves two component, a instance centric representation combining with a context aware representation.

For any instance  $\mathbf{x} \in \mathcal{X}_{\text{train}} \cup \mathcal{X}_{\text{test}}$ , we define its complementary set as  $\mathbf{x}^C$ . Then we implement the set transformation by:

$$\begin{aligned} \hat{\phi}(\mathbf{x}) &= \sum_{\mathbf{x}_{i'} \in \mathbf{x}^C} h(\phi(\mathbf{x}_{i'})) \\ \psi(\mathbf{x}) &= \phi(\mathbf{x}) + g([\phi(\mathbf{x}); \hat{\phi}(\mathbf{x})]) \end{aligned} \quad (14)$$

In Eq. 14,  $g$  and  $h$  are transformations which map the embedding into another space and increase the representation

ability of the embedding. In detail, we use two-layer fully connected neural networks with ReLU activation to implement these two mappings. The information of elements in the set is first combined into a vector  $\hat{\phi}(\mathbf{x})$ , then it is concatenated with the input embedding to obtain the embedding adaptation residual. This conditioned embedding takes the influence of other instances in the set into consideration, and keeps the “set” property. Finally, we determine the label with the newly adapted embedding  $\psi$  and Eq. 12. The result of this method can be found in Table 8

## B. Details of the Transformer

In this section, we provide details about the transformer component in our **Few-shot Embedding Adaptation with Transformer** (FEAT). Then we will introduce the setup for the transformer to extend to transductive and generalized Few-Shot Learning (FSL).

### B.1. Transformer for standard FSL

In this section, we describe in details about our **Few-Shot Embedding Adaptation via Transformer** (FEAT) approach, specifically how to use the Transformer architecture [43] to implement the set-to-set function  $\mathbf{T}$ , where self-attention mechanism facilitates the instance embedding adaptation with the contextual embeddings consideration.

Transformer is a store of triplets in the form of (query, key and value). Elements in the query set is the ones we want to do transformation. The transformer first match a query point with each of the keys by computing the “query” – “key” similarities. Then the proximity of the key to the query point is used to weight the corresponding values of each keys. The transformed input is served as a residual value which will be added over the input.

**Basic Transformer.** Following the definitions in [43], we use  $\mathcal{Q}$ ,  $\mathcal{K}$ , and  $\mathcal{V}$  to denote the set of query, keys, and values respectively. All these sets are implemented by different combination of task instances.

To increase the flexibility of the transformer, three sets of linear projections ( $W_Q \in \mathbb{R}^{d \times d'}$ ,  $W_K \in \mathbb{R}^{d \times d'}$ , and  $W_V \in \mathbb{R}^{d \times d'}$ ) are defined, one for each sets<sup>2</sup>. The points in sets are first projected by the corresponding projections

$$\begin{aligned} Q &= W_Q^\top [\phi_{\mathbf{x}_q}; \forall \mathbf{x}_q \in \mathcal{Q}] \in \mathbb{R}^{d' \times |\mathcal{Q}|} \\ K &= W_K^\top [\phi_{\mathbf{x}_k}; \forall \mathbf{x}_k \in \mathcal{K}] \in \mathbb{R}^{d' \times |\mathcal{K}|} \\ V &= W_V^\top [\phi_{\mathbf{x}_v}; \forall \mathbf{x}_v \in \mathcal{V}] \in \mathbb{R}^{d' \times |\mathcal{V}|} \end{aligned} \quad (15)$$

$|\mathcal{Q}|$ ,  $|\mathcal{K}|$ , and  $|\mathcal{V}|$  are the number of elements in the sets  $\mathcal{Q}$ ,  $\mathcal{K}$ , and  $\mathcal{V}$  respectively. Since there is a one-to-one correspondence between elements in  $\mathcal{K}$  and  $\mathcal{V}$  we have  $|\mathcal{K}| = |\mathcal{V}|$ .

<sup>2</sup>For notation simplicity, we omit the bias in the linear projection here.

The similarity between a query point  $\mathbf{x}_q \in \mathcal{Q}$  and the list of keys  $\mathcal{K}$  is then computed as “attention”:

$$\alpha_{qk} \propto \exp\left\{\left(\frac{\phi_{\mathbf{x}_q}^\top W_Q \cdot K}{\sqrt{d}}\right)\right\}; \forall \mathbf{x}_k \in \mathcal{K} \quad (16)$$

$$\alpha_{q,:} = \text{softmax}\left(\frac{\phi_{\mathbf{x}_q}^\top W_Q \cdot K}{\sqrt{d}}\right) \in \mathbb{R}^{|\mathcal{K}|} \quad (17)$$

The  $k$ -th element  $\alpha_{qk}$  in the vector  $\alpha_{q,:}$  reveals the particular proximity between  $\mathbf{x}_k$  and  $\mathbf{x}_q$ . The computed attention values are then used as weights for the final embedding  $\mathbf{x}_q$ :

$$\tilde{\psi}_{\mathbf{x}_q} = \sum_k \alpha_{qk} V_{:,k} \quad (18)$$

$$\psi_{\mathbf{x}_q} = \tau(\phi_{\mathbf{x}_q} + W_{\text{FC}}^\top \tilde{\psi}_{\mathbf{x}_q}) \quad (19)$$

$V_{:,k}$  is the  $k$ -th column of  $V$ .  $W_{\text{FC}} \in \mathbb{R}^{d' \times d}$  is the projection weights of a fully connected layer.  $\tau$  completes a further transformation, which is implemented by the dropout [40] and layer\_norm [4]. The whole flow of transformer in our FEAT approach can be found in Fig. 5. With the help of transformer, the embedding of each query instance is adapted.

**Multi-Head Multi-Layer Transformer.** Following [43], there exists an extended version of Transformer with stronger representation ability. Multiple sets of projections could be used in the attention. Assume there are totally  $H$  heads, the transformer concatenates the attention-transformed embedding first, and then uses a fully connected layer to project the embedding to the original embedding space. In detail,

$$\begin{aligned} \tilde{\psi}_{\mathbf{x}_q}^h &= \sum_k \alpha_{qk} V_{:,k}, & \forall h = 1, \dots, H \\ \hat{\psi}_{\mathbf{x}_q} &= \text{cat}(\tilde{\psi}_{\mathbf{x}_q}^h), & \forall h = 1, \dots, H \\ \psi_{\mathbf{x}_q} &= \tau(\phi_{\mathbf{x}_q} + W_{\text{FC}}^\top \hat{\psi}_{\mathbf{x}_q}) \end{aligned} \quad (20)$$

The concatenation operator  $\text{cat}$  makes the middle embedding as a  $d' \times H$  vector. Then the projection  $W_{\text{FC}} \in \mathbb{R}^{d' \times d}$  maps the embedding to the original space.  $\tau$  is the same configuration as before.

Besides, we can regard the transformer as an feature encoder of the input query point. Therefore, it can be applied over the input query point multiple times (with different sets of parameters), which gives rise to the multi-layer transformer. We will also discuss the multi-layer version with shared-parameter in Section D.

### B.2. Extension to transductive and generalized FSL

Facilitated by the flexible set transformer in Eq. 19, our adaptation approach can naturally extend to both the transductive and generalized settings.

When classifying test instance  $\mathbf{x}_{\text{test}}$  in the transductive scenario, other test instances  $\mathcal{X}_{\text{test}}$  from the  $N$  categories would also be available. Therefore, we enrich the transformer’s query and key/value sets

$$\mathcal{Q} = \mathcal{K} = \mathcal{V} = \mathcal{X}_{\text{train}} \cup \mathcal{X}_{\text{test}} \quad (21)$$

In this manner, the embedding adaptation procedure would also consider the structure among unlabeled test instances.

In the generalized few-shot classification, while  $\mathcal{D}_{\text{train}}$  still contains training instances from  $N$  UNSEEN classes, the set of test instances  $\mathcal{X}_{\text{test}}$  comes from both  $\mathcal{S}$  and the sampled  $N$  UNSEEN classes.

Not only to learn how to adapt embedding once novel classes present, in the generalized scenario, the model should also maintain the ability to classify SEEN classes by “memorizing” its discriminative ability over SEEN classes. Therefore, it requires to maintain the centers for all classes in  $\mathcal{S}$ , and learn  $\mathcal{C}$ . Assume that the class centers is maintained as a running mean embedding for each class (we denote them as a class centers set  $\mathcal{C}$ ), the resulted query and key/value sets of the transformer  $\mathcal{T}$  are:

$$\mathcal{Q} = \mathcal{K} = \mathcal{V} = \mathcal{X}_{\text{train}} \cup \mathcal{C} \cup \mathbf{x}_{\text{test}} \quad (22)$$

Assume there are  $|\mathcal{S}|$  classes in  $\mathcal{S}$ , after adapted with the seen class centers, all test instances are classified into  $N + |\mathcal{S}|$  classes.

The training objective for the generalized FSL is a bit different from the standard one. During the model learning, we need to mimic both the SEEN and UNSEEN classes for evaluation. More concretely, we first sample a  $M$ -shot  $N$ -way  $\mathcal{D}_{\text{train}}^{\mathcal{S}}$  from  $\mathcal{S}$ , then in addition to the corresponding  $\mathcal{D}_{\text{test}}^{\mathcal{S}}$ , we still sample 15 instances from each of the remaining  $|\mathcal{S}| - N$  classes and construct another test set  $\mathcal{D}_{\text{seen,test}}^{\mathcal{S}}$  to evaluate the model’s classification ability on the SEEN classes. The adapted embedding of each test instance is used to compute the similarity between  $\mathcal{D}_{\text{train}}^{\mathcal{S}}$  and  $\mathcal{C}$  to do a  $(\mathcal{S} + N)$ -way classification, where we mask out the loss of the selected  $N$  classes in  $\mathcal{C}$ .

## C. Implementation Details

**Backbone structure.** We consider two backbone convolutional networks as suggested in literature as instance embedding functions  $\mathbf{E}$  for the purpose of fair comparisons.

1) Four-layer convolution network (ConvNet) [39, 42, 44]. It contains 4 repeated convolutional blocks. In each block, there is a convolutional layer with  $3 \times 3$  kernel, a Batch Normalization layer [15], a ReLU, and a Max pooling with size 2. We resize the input image to  $84 \times 84 \times 3$ , and set the number of convolutional channels in each block as 64. A bit different from the literature, we add a global max pooling layer at last to reduce the dimensionality of the embedding. Based on the empirical observations, this

will not influence the results, but reduces the computation burden of later transformations a lot,

2) Wide residual network (ResNet) [30, 32, 37]. Following the literature, we resize the input image to  $80 \times 80 \times 3$ . Three residual blocks are used after an initial convolutional layer (with stride 1 and padding 1) over the image, which have channels 160/320/640, stride 2, and padding 2. After a global average pooling layer, it leads to a 640 dimensional embedding.

**Datasets.** Two datasets, *MiniImageNet* [44] and Caltech-UCSD Birds (CUB) 200-2011 [45] are investigated in this paper. Each dataset is split into three parts based on different non-overlapping sets of classes, for model training (a.k.a. meta-training in the literature), model validation, and model evaluation (a.k.a. meta-test in the literature). For all images in the CUB dataset, we use the provided bounding box to crop the images as a pre-processing [42]. Before input into the backbone network, all images are resized based on the requirement of the network.

**Pre-trained strategy.** As mentioned before, we applied an additional pre-training strategy as suggested in [32, 37]. The backbone network, appended with a softmax layer, is trained to classify all classes in the model learning split. The pre-trained weights are then used to initialize the embedding function  $\mathbf{E}$  in the few-shot learning. Based on [32]’s work, we investigate two pre-trained ways.

First, we learn a classifier on the model learning split with the cross-entropy loss. For example, a 64-way classifier is learned first over *MiniImageNet*. The last embedding layer (the layer before softmax) is used over the instances from the model validation split, and then the few-shot classification performance of the embedding layer is evaluated to select the best pre-trained model. The results based on this approach is shown in the main paper.

Second, we exactly follow the pre-trained way in [32] which takes full utilization of the data in model learning and validation splits, which achieves a higher results. We will include our results with this strategy in later sections.

**Transformer Parameters.** We follow the architecture as presented in [43] to build our FEAT and FEAT<sup>+</sup> models. The hidden dimension  $d'$  for the linear transformation in our FEAT model is set to be 64 for ConvNet and 640 for ResNet. The dropout rate is set as 0.5. We empirically observed that the shallow transformer (with one set of projection and one stacked layer) gives the best overall performance (also studied in Section D.2).

**Sampling strategy.** For FEAT<sup>+</sup>, we construct auxiliary set from  $\mathcal{X}_{\text{train}}^{\mathcal{S}}$  by sampling 2 instances from each class in

$S$ . It is notable that we only do forward computation over these auxiliary instances with no back propagation.

**Optimization.** Following the literature, different optimizers are used for these two backbones during the training. For the ConvNet backbone, stochastic gradient descent with Adam [16] optimizer is employed, with the initial learning rate set to be 1e-3. As the backbone network has been pre-trained, we scale the learning rate for those set of parameters by 0.1. For the ResNet backbone, valina stochastic gradient descent with Nesterov acceleration is used with an initial rate 0.0001. We will decrease the learning rate 10 times smaller after 10 epochs.

## D. Additional Experimental Results

In this section, we will show more experimental results over the *miniImageNet* dataset, the ablation studies, visualization, and extended few-shot learning.

### D.1. Main Results

The full results of all methods on the *MiniImageNet* can be found in Table 8. Comparing with the Table 1 in the main paper, here we add another two baselines. The first is MAML [10] optimized over the pre-trained embedding network. We re-implement the ConvNet backbone of MAML, and cite the MAML results over ResNet backbone from [37], which utilizes the same way of initialization. Another important baseline is the DeepSets [48] (denoted as DEEPSETS(ProtoNet) in the table), which is described concretely in Section A.

The adaptation via DeepSets also improves the results of the basic ProtoNet to some extent, and is more stable than the LSTM counterpart. For example, LSTM fails to enhance the embedding at 5-shot 5-way task with Resnet backbone, while DeepSets achieves higher performance than its baseline. It validates that using a set-to-set function as an embedding adaptation transformation is important.

We find the results of LEO [37] is updated in its newest version, so we also update the latest results of LEO in Table 8. Comparing with these results, our FEAT variants can still achieve the highest performance.

For our FEAT<sup>+</sup>, we construct an auxiliary set by sampling 2 instances from each of the SEEN classes. We test the performance when sampling more instances to enlarge the auxiliary set, but the results do not improve except the high computational burden. The main reason is that too many different-class instances may distract the attention and de-emphasis the same-class examples.

### D.2. Ablation Studies

#### Can FEAT generalize to more classes in the target tasks?

The 5-shot 5-way classification results can be found in

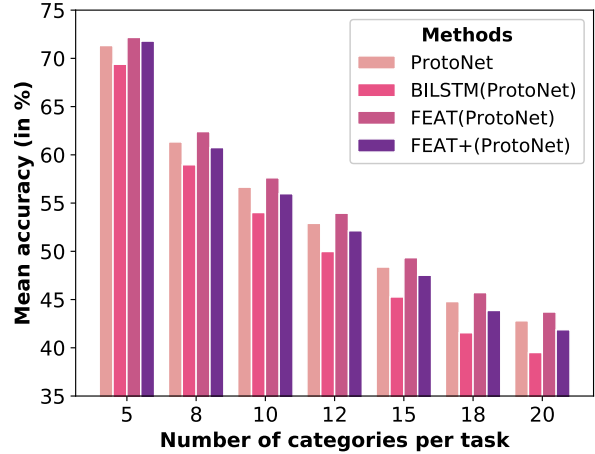


**Figure 6:** Five-shot learning accuracy when evaluated on more unseen tasks with larger number of classes ( $N=\{5, 8, 10, 12, 15, 18, 20\}$ ). Models are only trained for 5-way classification tasks.

Fig. 6. ProtoNet achieves higher performance in this case, while our FEAT still gets improvements in all configurations of  $N$ . FEAT<sup>+</sup> cannot always obtain the good results since the helpfulness of auxiliary instances is not obvious given more training examples.

**Will adapt multiple times helps?** The flexible transformer structure of FEAT is able to adapt the instance embedding *multiple* times in model evaluation [8]. In detail, we can apply the transformer embedding adaptation  $\mathbf{T}$  in Eq. 13 in a sequential way. It is notable that this multiple times embedding adaptation is different from the multi-layer extension of transformer. Here those different “layers” share the same parameters. The results can be found in Table 9. Adaptation with multiple times cannot help to improve the quality of the embedding. So using just one-layer transformer is the best choice in most cases.

**The effectiveness of CAL.** The results when the value of  $\lambda$  varies can be found in Table 10. From the results, we can find that the balance of CAL in the learning objective can influence the final results. Empirically, we set  $\lambda = 10$  in our experiments.

**The influence of the pre-trained features.** As we discussed before, there are two types of pre-trained strategies for the backbone network. We show the influence of the two pre-trained ways in Table 11. With pre-trained ways in [32], which takes full advantages of the dataset splits for model learning and validation, all methods achieve higher results. In this case, especially with ResNet backbone, our FEAT and FEAT<sup>+</sup> can still achieve the state-of-the-art performance.

**Table 8:** Few-shot classification accuracy  $\pm$  95% confidence interval on *MiniImageNet*. Our implementation methods are measured over 10,000 test trials.

Setups $\rightarrow$	1-Shot 5-Way		5-Shot 5-Way	
Backbone Network $\rightarrow$	ConvNet	ResNet	ConvNet	ResNet
MatchNet [44]	43.40 $\pm$ 0.78	-	51.09 $\pm$ 0.71	-
MAML [10]	48.70 $\pm$ 1.84	-	63.11 $\pm$ 0.92	-
ProtoNet [39]	49.42 $\pm$ 0.78	-	68.20 $\pm$ 0.66	-
RelationNet [41]	51.38 $\pm$ 0.82	-	67.07 $\pm$ 0.69	-
PFA [32]	54.53 $\pm$ 0.40	59.60 $\pm$ 0.41	67.87 $\pm$ 0.20	73.74 $\pm$ 0.19
TADAM [30]	-	58.50 $\pm$ 0.30	-	76.70 $\pm$ 0.30
LEO [37]	-	61.76 $\pm$ 0.08	-	77.59 $\pm$ 0.12
<b>Baselines</b>				
MAML	49.24 $\pm$ 0.21	58.05 $\pm$ 0.10	67.92 $\pm$ 0.17	72.41 $\pm$ 0.20
MatchNet	52.87 $\pm$ 0.20	60.66 $\pm$ 0.20	67.49 $\pm$ 0.17	75.05 $\pm$ 0.16
ProtoNet	52.61 $\pm$ 0.20	61.40 $\pm$ 0.20	71.33 $\pm$ 0.16	76.56 $\pm$ 0.16
BILSTM(MatchNet)	54.59 $\pm$ 0.20	59.36 $\pm$ 0.20	68.20 $\pm$ 0.16	72.98 $\pm$ 0.16
BILSTM(ProtoNet)	54.10 $\pm$ 0.20	55.73 $\pm$ 0.21	69.39 $\pm$ 0.16	69.93 $\pm$ 0.15
DEEPSETS(ProtoNet)	53.02 $\pm$ 0.20	60.06 $\pm$ 0.20	70.25 $\pm$ 0.16	77.95 $\pm$ 0.15
<b>Our approach</b>				
FEAT (MatchNet)	55.15 $\pm$ 0.20	60.08 $\pm$ 0.20	70.49 $\pm$ 0.16	77.87 $\pm$ 0.15
FEAT (ProtoNet)	55.21 $\pm$ 0.20	<b>62.60 <math>\pm</math> 0.20</b>	<b>72.17 <math>\pm</math> 0.16</b>	78.06 $\pm$ 0.15
FEAT <sup>+</sup> (MatchNet)	55.33 $\pm$ 0.20	60.92 $\pm$ 0.20	69.68 $\pm$ 0.16	76.35 $\pm$ 0.16
FEAT <sup>+</sup> (ProtoNet)	<b>55.79 <math>\pm</math> 0.20</b>	61.72 $\pm$ 0.20	71.79 $\pm$ 0.16	<b>78.38 <math>\pm</math> 0.15</b>

**Table 9:** The results of FEAT when adapt the embedding 1 – 3 times during model evaluation.

Setups $\rightarrow$	1-Shot 5-Way	5-Shot 5-Way
1	<b>55.21 <math>\pm</math> 0.20</b>	<b>72.17 <math>\pm</math> 0.16</b>
2	55.00 $\pm$ 0.20	71.47 $\pm$ 0.16
3	54.98 $\pm$ 0.20	70.44 $\pm$ 0.16

**Table 10:** Ablation studies on effects of regularization.

Setups $\rightarrow$	1-Shot 5-Way	5-Shot 5-Way
FEAT(ProtoNet)	54.65 $\pm$ 0.20	71.47 $\pm$ 0.16
FEAT <sup>+</sup> (ProtoNet)	55.39 $\pm$ 0.11	70.99 $\pm$ 0.16
$\lambda = 1.0$		
FEAT(ProtoNet)	55.19 $\pm$ 0.20	71.77 $\pm$ 0.16
FEAT <sup>+</sup> (ProtoNet)	54.70 $\pm$ 0.19	71.39 $\pm$ 0.16
$\lambda = 10.0$		
FEAT(ProtoNet)	55.21 $\pm$ 0.20	<b>72.17 <math>\pm</math> 0.16</b>
FEAT <sup>+</sup> (ProtoNet)	<b>55.79 <math>\pm</math> 0.11</b>	71.79 $\pm$ 0.16
$\lambda = 100.0$		
FEAT(ProtoNet)	54.92 $\pm$ 0.20	71.83 $\pm$ 0.16
FEAT <sup>+</sup> (ProtoNet)	54.37 $\pm$ 0.20	69.45 $\pm$ 0.16

**Two implementations of the 5-Shot embedding adaptation based on the ProtoNet.** ProtoNet classifies a test in-

stance based on the label of the nearest class center. There are two embedding adaptation variants in this implementation when there are more than one instance in each class, *i.e.*, we can compute the class center before or after the embedding adaptation. In other words, the class prototype in Eq. 12 can be computed based on  $\phi(\mathbf{x})$  or  $\psi(\mathbf{x})$ . In our experiments, we use the former strategy for 5-shot tasks to get the class centers.

From empirical results, we find there dose not exist an obvious difference between these two strategies. For FEAT (ProtoNet) with the later computation strategy, it achieves  $72.08 \pm 0.20$  on 5-shot 5-way tasks.

### D.3. Qualitative Visualization of Attention

Here we show more results of selected helpful instances when we apply the FEAT<sup>+</sup> in Fig. 7. Different tasks are divided by the tables. In a particular task, we show the training set instances with labels in the first row, the image of test instance and the selected most helpful instances from the sampled auxiliary set (sorted by their attention value in a descending order) in the following rows. Based on these results, we find the FEAT<sup>+</sup> is helpful especially the task is very difficult, *e.g.* the few-shot training set cannot reveal the discriminative characteristics of the classes. In this case, the FEAT<sup>+</sup> can utilize some related instances in the sampled set from the seen classes to help adapt the instance embeddings.

**Table 11:** Few-shot classification accuracy  $\pm$  95% confidence interval on *MiniImageNet*, with two different backbone network pre-trained strategies. Our implementation methods are measured over 10,000 test trials.

Setups →	1-Shot 5-Way		5-Shot 5-Way	
Backbone Network →	ConvNet	ResNet	ConvNet	ResNet
<b>with pre-training strategy of [37]</b>				
LEO [37]	-	61.76 $\pm$ 0.05	-	77.59 $\pm$ 0.12
ProtoNet	52.61 $\pm$ 0.20	61.40 $\pm$ 0.20	71.33 $\pm$ 0.16	76.56 $\pm$ 0.16
BILSTM(ProtoNet)	54.10 $\pm$ 0.20	55.73 $\pm$ 0.21	69.39 $\pm$ 0.16	69.93 $\pm$ 0.15
FEAT (ProtoNet)	55.21 $\pm$ 0.20	<b>62.60 <math>\pm</math> 0.20</b>	<b>72.17 <math>\pm</math> 0.16</b>	78.06 $\pm$ 0.15
FEAT <sup>+</sup> (ProtoNet)	<b>55.79 <math>\pm</math> 0.20</b>	61.72 $\pm$ 0.20	71.79 $\pm$ 0.16	<b>78.38 <math>\pm</math> 0.15</b>
<b>with pre-training strategy of [32]</b>				
PFA [32]	54.53 $\pm$ 0.40	59.60 $\pm$ 0.41	67.87 $\pm$ 0.20	73.74 $\pm$ 0.19
LEO [37]	-	63.97 $\pm$ 0.20	-	79.49 $\pm$ 0.70
ProtoNet	53.32 $\pm$ 0.20	61.98 $\pm$ 0.21	72.65 $\pm$ 0.16	79.46 $\pm$ 0.16
BILSTM(ProtoNet)	55.82 $\pm$ 0.20	59.03 $\pm$ 0.21	69.43 $\pm$ 0.16	71.78 $\pm$ 0.18
FEAT (ProtoNet)	<b>57.02 <math>\pm</math> 0.20</b>	63.96 $\pm$ 0.20	<b>73.26 <math>\pm</math> 0.16</b>	80.28 $\pm$ 0.15
FEAT <sup>+</sup> (ProtoNet)	56.56 $\pm$ 0.20	<b>64.60 <math>\pm</math> 0.20</b>	72.89 $\pm$ 0.16	<b>80.33 <math>\pm</math> 0.14</b>

**Table 12:** Results of models for transductive FSL with ConvNet backbone on *MiniImageNet*.

Setups →	1-Shot 5-Way	5-Shot 5-Way
<b>Standard</b>		
ProtoNet	52.61 $\pm$ 0.20	71.33 $\pm$ 0.16
FEAT (ProtoNet)	55.21 $\pm$ 0.20	72.17 $\pm$ 0.16
<b>Transductive</b>		
Semi-ProtoNet [35]	50.41 $\pm$ 0.31	64.39 $\pm$ 0.24
TPN [26]	54.72 $\pm$ 0.84	69.25 $\pm$ 0.67
FEAT(ProtoNet)	<b>56.49 <math>\pm</math> 0.21</b>	<b>72.65 <math>\pm</math> 0.16</b>
FEAT <sup>+</sup> (ProtoNet)	55.40 $\pm$ 0.20	70.16 $\pm$ 0.67

#### D.4. More Transductive FSL Discussions

We list the result of transductive few-shot classification in Table 12, where the unlabeled test instances arrive simultaneously when classifying a test instance. We compare with two previous approaches, Semi-ProtoNet [35] and TPN [26]. Semi-ProtoNet utilizes the unlabeled instances in the prototypical network determination, while TPN meta learns a label propagation way to take unlabeled instances relationship into consideration. We cite their results over *miniImageNet* directly as a reference.

In this setting, our model leverage the unlabeled test instances to augment the transformer as discussed in Sec. B.1, and the embedding adaptation takes relationship of all test instances into consideration. From the results, FEAT achieves further performance improvement compared with standard setting. The performance gain induced by the transductive FEAT (ProtoNet) is more significant in the one-shot learning setting comparing to the five-shot scenario,

**Table 13:** Results of generalized FEAT variants with ConvNet backbone on *MiniImageNet*. All methods are evaluated on instances composed by SEEN classes, UNSEEN classes, and both of them (JOINT), respectively.

Measures →	SEEN	UNSEEN	JOINT
<b>1-shot learning</b>			
ProtoNet	41.73 $\pm$ 0.03	48.64 $\pm$ 0.20	35.69 $\pm$ 0.03
FEAT(ProtoNet)	43.94 $\pm$ 0.03	<b>49.72 <math>\pm</math> 0.20</b>	40.50 $\pm$ 0.03
FEAT <sup>+</sup> (ProtoNet)	<b>47.28 <math>\pm</math> 0.03</b>	48.08 $\pm$ 0.19	<b>43.50 <math>\pm</math> 0.03</b>
<b>5-shot learning</b>			
ProtoNet	41.06 $\pm$ 0.03	64.94 $\pm$ 0.17	38.04 $\pm$ 0.02
FEAT(ProtoNet)	44.94 $\pm$ 0.03	<b>65.33 <math>\pm</math> 0.16</b>	41.68 $\pm$ 0.03
FEAT <sup>+</sup> (ProtoNet)	<b>47.43 <math>\pm</math> 0.03</b>	65.00 $\pm$ 0.19	<b>44.10 <math>\pm</math> 0.03</b>
Random Chance	1.56	20.00	1.45

since the helpfulness of unlabeled instance decreases when there are more labeled instances. We empirically find the additional sampled auxiliary instances in this transductive setting distract the attention, so that the last performance of transductive FEAT<sup>+</sup> does not improve.

#### D.5. More Generalized FSL Results

Considering the computational burden, we reduce the number of test instances per class during model learning to 5 (but there are still 15 instances per class for model evaluation). Here we show the full results of FEAT and FEAT<sup>+</sup> in the generalized few-shot learning setting in Table 13, which includes both the 1-shot and 5-shot performance. In the 5-shot scenario, the performance improvement mainly come from the improvement of over the UNSEEN tasks.

Training instance	Nematode	Mixing bowl	Cuirass	Golden retriever	Ant
Test instance					
Golden retriever	Arctic fox	Tibetan mastiff	Komondor	Miniature poodle	Newfoundland
	0.0598	0.0550	0.0468	0.0445	0.0417
Cuirass	Reel	Chime	Tibetan mastiff	Triceratops	Stage
	0.0259	0.0251	0.0227	0.0260	0.0253
Training instance	Electric guitar	Dalmatian	Lion	Hourglass	Nematode
Test instance					
Dalmatian	Miniature poodle	File	Tibetan mastiff	Cocktail shaker	Unicycle
	0.0799	0.0328	0.0211	0.0208	0.0199
Lion	Komondor	Boxer	Unicycle	Miniature poodle	Barrel
	0.0287	0.0264	0.0256	0.0207	0.0205
Training instance	Golden retriever	Mixing bowl	Ferret	Electric guitar	King crab
Test instance					
Electric guitar	Dishrag	Pencil box	Slot	Cocktail shaker	Dishrag
	0.0397	0.0395	0.0356	0.0311	0.0241
Electric guitar	Stage	Gordon setter	Slot	Lipstick	Prayer rug
	0.0414	0.0376	0.0313	0.0195	0.0181
Training instance	Trifle	Mixing bowl	Hunting dog	Nematode	School Bus
Test instance					
Mixing bowl	Jellyfish	Jellyfish	Dugong	Dugong	Komondor
	0.0581	0.0468	0.0465	0.347	0.0193
Nematode	Organ	Cocktail shaker	Jellyfish	Lipstick	Photocopier
	0.0416	0.0310	0.0275	0.024	0.022
Training instance	Lion	Hunting dog	School Bus	Vase	Electric guitar
Test instance					
School Bus	Street sign	Chime	Tobacco shop	Tobacco shop	Parallel bars
	0.0428	0.0389	0.0354	0.0327	0.0297
Vase	Consomme	Consomme	Hotdog	Orange	Jellyfish
	0.0447	0.0226	0.0171	0.0164	0.0157

**Figure 7:** The embedding adaptation facilitated instances selected by FEAT<sup>+</sup> in two tasks (related instances come first). Texts above/below images are the labels and the value of attention.